Impaired endothelium-mediated cerebrovascular reactivity promotes anxiety and respiration disorders in mice

Jan Wenzel[a,b,1], Cathrin E. Hansen[a], Carla Bettoni[c], Miriam A. Vogt[d], Beate Lembrich[a], Rentsenkhand Natsagdorj[a,b], Gianna Huber[a], Josefine Brands[a,b], Kjestine Schmidt[b,e], Julian C. Assmann[a], Ines Stölting[a], Kathrin Saar[f,g], Jan Sedlacik[h], Jens Fiehler[h], Peter Ludewig[i], Michael Wegmann[j], Nina Feller[a], Marius Richter[a], Helge Müller-Fielitz[a], Thomas Walther[a], Gabriele M. König[k], Evi Kostenis[k], Walter Raasch[a,b], Norbert Hübner[f,g,l], Peter Gass[d], Stefan Offermanns[m], Cor de Wit[b,e], Carsten A. Wagner[c], and Markus Schwaninger[a,b,1]

[a]Institute for Experimental and Clinical Pharmacology and Toxicology, University of Lübeck, 23562 Lübeck, Germany; [b]DZHK (German Research Centre for Cardiovascular Research), partner site Hamburg/Lübeck/Kiel, 23562 Lübeck, Germany; [c]Institute of Physiology, University of Zürich, CH-8057 Zürich, Switzerland; [d]Central Institute of Mental Health, Medical Faculty of Mannheim/University of Heidelberg, 68159 Mannheim, Germany; [e]Institute of Physiology, University of Lübeck, 23562 Lübeck, Germany; [f]Cardiovascular and Metabolic Sciences, Max Delbrück Center for Molecular Medicine in the Helmholtz Association, 13125 Berlin, Germany; [g]DZHK (German Research Centre for Cardiovascular Research), partner site Berlin, 13125 Berlin, Germany; [h]Department of Diagnostic and Interventional Neuroradiology, University Medical Center Hamburg-Eppendorf, 20251 Hamburg, Germany; [i]Department of Neurology, University Medical Center Hamburg-Eppendorf, 20251 Hamburg, Germany; [j]Priority Area Asthma and Allergy, Research Center Borstel, 23845 Borstel, Germany; [k]Institute for Pharmaceutical Biology, University of Bonn, 53115 Bonn, Germany; [l]Charité Universitätsmedizin Berlin, 10117 Berlin; and [m]Department of Pharmacology, Max Planck Institute for Heart and Lung Research, 61231 Bad Nauheim, Germany

Edited by Louis J. Ignarro, University of California, Los Angeles School of Medicine, Beverly Hills, CA, and approved December 9, 2019 (received for review May 7, 2019)

Carbon dioxide (CO_2), the major product of metabolism, has a strong impact on cerebral blood vessels, a phenomenon known as cerebrovascular reactivity. Several vascular risk factors such as hypertension or diabetes dampen this response, making cerebrovascular reactivity a useful diagnostic marker for incipient vascular pathology, but its functional relevance, if any, is still unclear. Here, we found that GPR4, an endothelial H^+ receptor, and endothelial $G\alpha_{q/11}$ proteins mediate the CO_2/H^+ effect on cerebrovascular reactivity in mice. CO_2/H^+ leads to constriction of vessels in the brainstem area that controls respiration. The consequential washout of CO_2, if cerebrovascular reactivity is impaired, reduces respiration. In contrast, CO_2 dilates vessels in other brain areas such as the amygdala. Hence, an impaired cerebrovascular reactivity amplifies the CO_2 effect on anxiety. Even at atmospheric CO_2 concentrations, impaired cerebrovascular reactivity caused longer apneic episodes and more anxiety, indicating that cerebrovascular reactivity is essential for normal brain function. The site-specific reactivity of vessels to CO_2 is reflected by regional differences in their gene expression and the release of vasoactive factors from endothelial cells. Our data suggest the central nervous system (CNS) endothelium as a target to treat respiratory and affective disorders associated with vascular diseases.

endothelial dysfunction | brain endothelial cells | hypercapnia | respiration | anxiety

Cerebral blood flow (CBF) supplies energy substrates to the brain and removes metabolic products. Therefore, CBF is tightly controlled (1, 2). Since the 19th century, it has been known that carbon dioxide $(CO_2)/H^+$ is one of the strongest stimuli for increasing brain perfusion (3–5). While it may seem plausible that as the major product of metabolism CO_2 increases CBF to enhance its removal and replenish nutrients, a physiological function of cerebrovascular reactivity to CO_2 has never been proven experimentally. Also, the molecular mechanisms underlying cerebrovascular reactivity are still debated. This lack of knowledge is surprising because many patients suffering from neurological, cardiovascular, and metabolic diseases show major alterations in cerebrovascular reactivity. In fact, cerebrovascular reactivity is routinely monitored as a diagnostic marker to detect early stages of vascular pathology (6). In the context of the multifaceted conditions associated with vascular risk factors, it has been difficult to delineate the functional consequences of impaired cerebrovascular reactivity. Therefore, we have investigated the mechanisms underlying CO_2-induced perfusion changes in the brain. Based on the obtained knowledge, we were able to selectively interfere with cerebrovascular reactivity and unexpectedly found that its integrity is required for the regulation of respiration and emotional behavior.

Results

CO_2-Induced CBF Response Depends Partially on GPR4. As an important mediator of the neuronal response to CO_2/H^+, ATP is released by erythrocytes (7) and parenchymal cells (8). ATP regulates the diameter of cerebral arterioles by acting on purinergic P_2Y receptors, including P_2Y_2, in endothelial and smooth muscle cells of the brain (9–11). Therefore, we examined the effect of

Significance

The ability of blood vessels to respond to endogenous and exogenous stimuli is of high importance. Several diseases lead to an impairment of vascular reactivity, especially in the brain. Here, we show that the functional consequences of impaired cerebrovascular reactivity differ between brain areas and depend on whether vessels constrict or dilate as a response to CO_2. A loss of vascular reactivity to carbon dioxide induces anxiety and changes respiration, even at a basal state. Area-specific vascular responses can be explained by characteristic gene expression patterns and release of vasoactive mediators.

Author contributions: J.W. and M.S. designed research; J.W., C.E.H., C.B., M.A.V., B.L., R.N., G.H., J.B., K. Schmidt, J.C.A., I.S., K. Saar, J.S., P.L., N.F., M.R., H.M.-F., and T.W., performed research; J.F., M.W., G.M.K., E.K., W.R., N.H., P.G., S.O., C.d.W., and C.A.W. contributed new reagents/analytic tools; J.W., C.E.H., C.B., M.A.V., R.N., G.H., J.B., K. Schmidt, J.C.A., K. Saar, H.M.-F., and C.A.W. analyzed data; and J.W. and M.S. wrote the paper.

The authors declare no competing interest.

This article is a PNAS Direct Submission.

Data deposition: Microarray data have been deposited in the ArrayExpress database at EMBL-EBI (https://www.ebi.ac.uk/arrayexpress/) under accession no. E-MTAB-8521.

[1]To whom correspondence may be addressed. Email: jan.wenzel@uni-luebeck.de or markus.schwaninger@uni-luebeck.de.

This article contains supporting information online at https://www.pnas.org/lookup/suppl/doi:10.1073/pnas.1907467117/-/DCSupplemental.

First published January 2, 2020.

deleting brain endothelial P_2Y_2 on CO_2-induced cerebral perfusion. We generated a mouse line that carries the brain endothelial-specific cre driver *Slco1c1-CreER*^{T2} (12) combined with a loxP-flanked P_2Y_2 gene (13) to delete this receptor selectively in the brain endothelium (*P2ry2*^{beKO} mice) and confirmed the knockout by using mRNA quantification and calcium imaging in primary forebrain endothelial cells (PFBECs) (14) (*SI Appendix*, Fig. S1 *A* and *B*). To investigate the effect of CO_2 on CBF, mice were artificially ventilated with normal air or a gas mix containing increased CO_2 concentrations without changing oxygen levels. CBF was measured by laser speckle imaging. CO_2 induced a similar increase in cortical perfusion of control and *P2ry2*^{beKO} mice (Fig. 1 *A* and *B*). Thus, the endothelial P_2Y_2 receptor is not involved in increasing cortical blood flow upon CO_2 exposure. Therefore, we tested the alternative hypothesis that CO_2/H^+ could be directly sensed by specific receptor proteins in the brain vasculature. In buffered biological systems, CO_2 is rapidly converted into protons and bicarbonate. Protons mediate most of the physiological effects of CO_2, such as respiratory stimulation (15) or fear responses (16). In addition, cerebral perfusion reacts to acidosis with strong vasodilation. Recently, several groups reported that some orphan G protein-coupled receptors (GPCRs) were activated by H^+ in a narrow physiological range (17, 18). Among them, GPR4 and GPR68 are expressed in vessels (18, 19). To examine the role of H^+ sensing by GPCRs during a CO_2-induced CBF increase, we investigated knockout mice for each of the receptors (15). GPR4

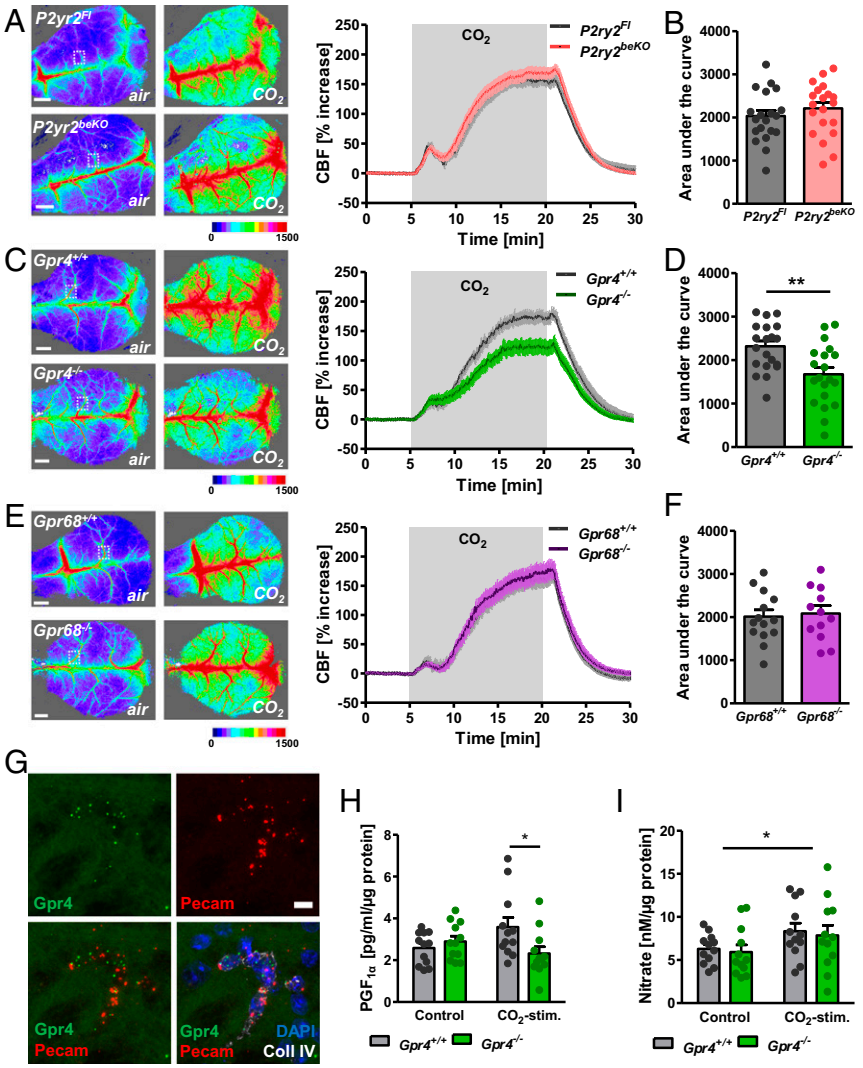

Fig. 1. GPR4 mediates CO_2-induced perfusion increase in the cortex. (*A*) Representative images taken before (air) and during CO_2 stimulation, and quantification of laser speckle imaging measuring cortical perfusion of *P2yr2*^{beKO} and control mice during artificial ventilation with 20% CO_2. An exemplary region of analysis is indicated by the white dotted box. (*B*) Areas under the curves shown in *A*; $n = 19$ to 20 mice per group. (*C*) Representative images taken before (air) and during CO_2 stimulation, and quantification of laser speckle imaging of *Gpr4*$^{-/-}$ and control mice during artificial ventilation with 20% CO_2. An exemplary region of analysis is indicated by the white dotted box. (*D*) Areas under the curves shown in *C*. Student's *t* test, $^{**}P < 0.01$; $n = 20$ mice per group. (*E*) Representative images taken before (air) and during CO_2 stimulation, and quantification of laser speckle imaging of *Gpr68*$^{-/-}$ and control mice during artificial ventilation with 20% CO_2. An exemplary region of analysis is indicated by the white dotted box. (*F*) Areas under the curves shown in *E*; $n = 12$ to 14 mice per group. (*G*) In situ hybridization of *Gpr4* mRNA shows coexpression with the endothelial cell marker *Pecam* and colocalization with the basement membrane protein collagen IV. (Scale bar, 10 µm.) The figure is a magnified image of *SI Appendix*, Fig. S1*E*. (*H*) $PGF_{1\alpha}$ as a surrogate for prostacyclin release of PFBECs of *Gpr4*$^{-/-}$ and control mice after 30-min stimulation with 5% (control) or 15% CO_2. $^{*}P < 0.05$ (2-way ANOVA with Bonferroni posttest); $n = 12$ per group. (*I*) Assessment of NO release by measurement of nitrate concentrations in the supernatant of PFBECs of *Gpr4*$^{-/-}$ and control mice after 30-min stimulation with 5% (control) or 15% CO_2. $^{*}P < 0.05$ (2-way ANOVA with Bonferroni posttest); $n = 12$ per group. Data are means ± SEM. Color scales in *A*, *C*, and *E* indicate arbitrary units of laser speckle images. (Scale bars in *A*, *C*, and *E*, 1 mm.).

knockout decreased CO_2-induced blood flow stimulation (Fig. 1 *C* and *D*), whereas we found no effect of the deletion of GPR68 on this response (Fig. 1 *E* and *F*). In the periphery, GPR68 is mainly expressed in smooth muscle cells while GPR4 has been mostly detected in endothelial cells, also in the brain (18–20). In line with the described localization, we detected GPR68 expression in brain vessel fragments containing smooth muscle cells, pericytes, and endothelial cells, but not in PFBECs (*SI Appendix*, Fig. S1*C*), whereas GPR4 was enriched in both vessel fragments and PFBECs compared to whole-brain lysate (*SI Appendix*, Fig. S1*D*). In situ hybridization confirmed that Gpr68 mRNA is colocalized with smooth muscle cells in vessels of the brain (*SI Appendix*, Fig. S1*F*), whereas Gpr4 mRNA is colocalized mainly with endothelial cells in brain tissue (Fig. 1*G* and *SI Appendix*, Fig. S1*E*). In contrast to previous reports on another GPR4 knockout mouse line (21), we did not observe any morphological changes of the brain microvasculature (*SI Appendix*, Fig. S1 *G* and *H*).

The involvement of GPR4 implies that increased CO_2/H^+ concentrations are sensed by endothelial rather than by smooth muscle cells. To characterize the endothelial signaling pathway, we stimulated PFBECs with increased CO_2 in a physiological, bicarbonate-buffered solution, lowering the pH to ∼7.0. We measured $PGF_{1\alpha}$ and nitrate as stable products of the endothelial-derived vasodilating mediators prostacyclin and nitric oxide (NO) and found both to be increased upon CO_2 exposure (Fig. 1 *H* and *I*). Prostacyclin release but not NO release was dependent on GPR4, indicating more than one mechanism by which CO_2 induces vasodilation via endothelial cells. GPR4 is able to induce $G\alpha_s$- and cAMP- as well as $G\alpha_{q/11}$-mediated signaling pathways (18, 22, 23). Unexpectedly, CO_2 did not increase, but rather decreased cAMP production in PFBECs (*SI Appendix*, Fig. S2*A*), indicating another mechanism in the brain endothelium, such as coupling to $G\alpha_{q/11}$ pathways (23). Indeed, we observed a similar decrease in prostacyclin release when we treated PFBECs with a specific and effective inhibitor of $G\alpha_{q/11}$ signaling (*SI Appendix*, Fig. S2 *B* and *C*). Additionally, by blocking this pathway the NO release was reduced in PFBECs after stimulation with CO_2 (24) (*SI Appendix*, Fig. S2*D*).

To verify the involvement of $G\alpha_{q/11}$ proteins, we used a strategy that was applied successfully in previous studies (13) and is based on the parallel deletion of *Gna11* and *Gnaq* as the respective gene products are able to compensate for each other. We combined a *Gna11* knockout, loxP-flanked *Gnaq* alleles (13), and the brain endothelial-specific *Slco1c1*-$CreER^{T2}$ driver (12), leading to a tamoxifen-inducible knockout of $G\alpha_{q/11}$ in brain endothelial cells ($G\alpha_{q/11}^{beKO}$ mice). We confirmed the deletion by quantifying *Gnaq* mRNA levels (*SI Appendix*, Fig. S3*A*) and intracellular Ca^{2+} concentrations in PFBECs in response to ATP (*SI Appendix*, Fig. S3*B*). As seen with the $G\alpha_{q/11}$ inhibitor, the increase of prostacyclin and NO release upon CO_2 stimulation was clearly reduced in PFBECs of $G\alpha_{q/11}^{beKO}$ mice compared to controls (*SI Appendix*, Fig. S3 *C* and *D*). Supporting the involvement of NO, the endothelial NO synthase (eNOS) was phosphorylated by CO_2 and this activation was impaired in PFBECs of $G\alpha_{q/11}^{beKO}$ animals (*SI Appendix*, Fig. S3*E*). Overall, the data suggest that CO_2/H^+ increase cortical CBF via the endothelial H^+-sensitive receptor GPR4, intracellular $G\alpha_{q/11}$ proteins, and the release of prostacyclin and NO.

CO_2-Induced CBF Response Depends on Endothelial $G\alpha_{q/11}$ Signaling. To investigate the role of endothelial $G\alpha_{q/11}$ signaling in the CO_2/H^+-induced cerebrovascular response in vivo, we used a gas mix containing 10% or 20% CO_2 to ventilate $G\alpha_{q/11}^{beKO}$ mice. These stimuli profoundly increased arterial pCO_2 and reduced arterial pH with no difference between genotypes (*SI Appendix*, Fig. S4 *A*–*C*). At a basal state, we did not find any changes in venous blood gases in $G\alpha_{q/11}^{beKO}$ mice (*SI Appendix*, Fig. S4 *D*–*F*). The brain endothelial-specific $G\alpha_{q/11}$ deletion interfered with the CO_2-induced CBF increase to an even greater extent than *Gpr4* knockout (Fig. 2 *A*–*E*). After a shorter stimulus of 10% CO_2 there was almost no effect of CO_2 on cortical perfusion in $G\alpha_{q/11}^{beKO}$ mice (*SI Appendix*, Fig. S4 *G* and *H*). In addition, endogenously induced CO_2/H^+ elevation via hypoventilation increased CBF in control mice but less so in $G\alpha_{q/11}^{beKO}$ animals (*SI Appendix*, Fig. S4 *I* and *J*). Even short apneic periods (3 s) markedly increased CBF in control mice but less so in $G\alpha_{q/11}^{beKO}$ animals (Fig. 2 *F*–*I*). In contrast, the whole-genome knockout of only *Gna11* did not affect cortical CO_2-induced perfusion (*SI Appendix*, Fig. S4 *K* and *L*). As deleting $G\alpha_{q/11}$ in all endothelial cells of the body, using another cre mouse line, induced arterial hypertension (13)—which has been shown to be a confounding factor in CBF studies—we examined the blood pressure in $G\alpha_{q/11}^{beKO}$ mice using telemetry. In contrast to the global endothelial deletion, the brain endothelial-specific deletion of $G\alpha_{q/11}$ in $G\alpha_{q/11}^{beKO}$ mice did not affect blood pressure or heart rate (*SI Appendix*, Fig. S4 *M* and *N*).

Laser speckle imaging is not suitable for measuring absolute perfusion in tissues. Therefore, we used arterial spin labeling MRI to quantify brain perfusion. We did not detect a difference in brain perfusion between $G\alpha_{q/11}^{beKO}$ and control mice (Fig. 2 *J* and *K*), which suggests that endothelial $G\alpha_{q/11}$ signaling may not play a role in the unstimulated cerebrovascular tone, at least during anesthesia. However, CO_2 exposure again led to a prominent increase in cerebral perfusion in control mice and this effect was diminished in $G\alpha_{q/11}^{beKO}$ animals (Fig. 2 *J* and *L*). The impaired vascular reactivity in $G\alpha_{q/11}^{beKO}$ mice is stimulus-specific because the CBF response to the vasodilatory anesthetic isoflurane did not differ between $G\alpha_{q/11}^{beKO}$ and control mice, in contrast to the response to CO_2 (*SI Appendix*, Fig. S4*O*). An unchanged vessel density and normal coverage of cortical vessels by pericytes, smooth muscle cells, and basement membrane proteins (*SI Appendix*, Fig. S5 *A*–*F*) support the finding that endothelial $G\alpha_{q/11}$ signaling is not necessary for baseline perfusion or normal vessel morphology in the brain, but is essential for the reactivity to CO_2/H^+.

Cerebral arterioles have been reported to dilate upon CO_2/H^+ (25). To investigate individual vessels, we generated acute cortical brain slices and measured CO_2/H^+-induced diameter changes in arterioles by using a method described recently (26). As expected from the above data, the deletion of endothelial $G\alpha_{q/11}$ signaling led to a loss of CO_2-induced arteriolar vessel dilation in cortical brain slices (Fig. 2 *M*–*O*), whereas normal reactivity was observed upon calcium withdrawal and exposure to a high concentration of potassium (*SI Appendix*, Fig. S5 *G* and *H*), demonstrating that the reduced response to CO_2/H^+ was not due to a general morphological or functional impairment of vessel reactivity. In support of this, diameters of unstimulated arterioles were not altered in cortical slices of $G\alpha_{q/11}^{beKO}$ mice (Fig. 2*P*). Taken together, our data indicate that endothelial cells play a critical role during CO_2-induced blood flow responses in the brain as they are able to sense H^+ changes by GPR4 and $G\alpha_{q/11}$ signaling and mediate the subsequent vascular reaction.

Impaired Vascular Reactivity to CO_2 Aggravates CO_2-Evoked Fear Response. Having established a mouse model of impaired cerebrovascular reactivity, we were able to investigate the physiological functions of CO_2/H^+-induced perfusion changes. Elevated CO_2 concentrations elicit several behavioral and respiratory responses that help lower CO_2 in the body. As a prominent effect, CO_2 leads to what has been interpreted as a suffocation alarm (27), consisting of fear and panic reactions in mice and humans by activating chemosensitive brain areas, including the basolateral amygdala (16). To investigate cerebrovascular reactivity in the amygdala, we prepared acute brain slices of this area and measured arteriolar diameter changes after a CO_2 stimulus. Again, as seen in cortical slices before, elevated CO_2 concentrations increased vessel diameters, a response that was almost absent in slices of $G\alpha_{q/11}^{beKO}$ mice

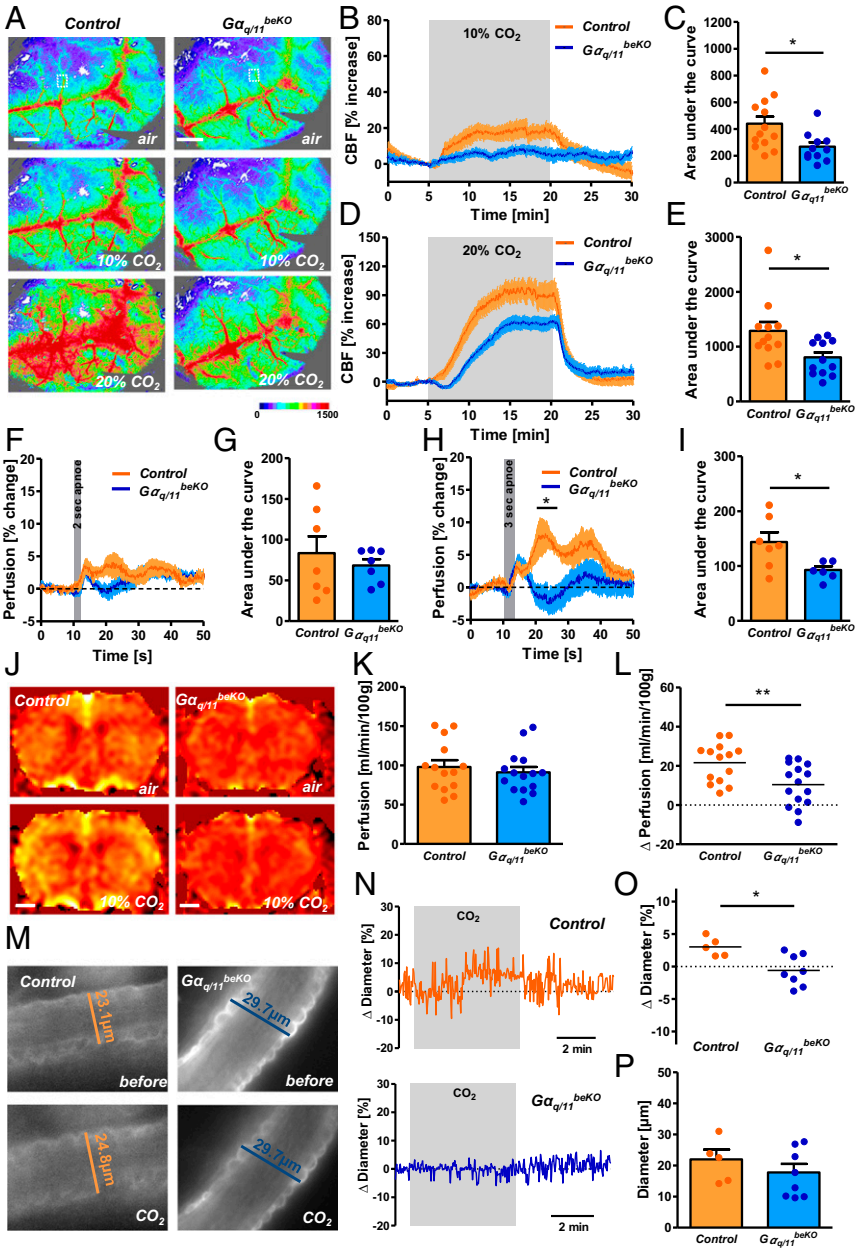

Fig. 2. Endothelial $G\alpha_{q/11}$ signaling mediates CO_2-induced perfusion increase in the cortex. (*A*) Representative images of laser speckle recordings of $G\alpha_{q/11}^{beKO}$ and control mice ventilated with different CO_2 concentrations taken before (air) and during CO_2 stimulation. Color scale indicates arbitrary units. An exemplary region of analysis is indicated by the white dotted box. (Scale bars, 1 mm.) (*B* and *D*) Quantification of laser speckle imaging measuring cortical perfusion of $G\alpha_{q/11}^{beKO}$ and control mice during artificial ventilation with 10% CO_2 (*B*) or 20% CO_2 (*D*). (*C* and *E*) Areas under the curves shown in *B* or *D*, respectively. Mann–Whitney *U* test, $^*P < 0.05$; $n = 11$ to 13 mice per group. (*F* and *H*) Quantification of laser speckle imaging measuring cortical perfusion of $G\alpha_{q/11}^{beKO}$ and control mice during and after short apneic periods of 2 (*F*) or 3 (*H*) seconds. $^*P < 0.05$ (RM-ANOVA with Bonferroni posttest); $n = 6$ to 7 mice per group. (*G* and *I*) Areas under the curves shown in *F* or *H*, respectively. Mann–Whitney *U* test, $^*P < 0.05$; $n = 6$ to 7 mice per group. (*J*) Representative images of arterial spin labeling (ASL)-MRI of $G\alpha_{q/11}^{beKO}$ and control mice before (air) and during stimulation with 10% CO_2. (*K*) Quantification of ASL-MRI perfusion measurements in the cortex of unstimulated $G\alpha_{q/11}^{beKO}$ and control mice; $n = 14$ to 15 mice per group. (*L*) Difference in ASL-MRI perfusion measurements in the cortex of CO_2-exposed and unexposed $G\alpha_{q/11}^{beKO}$ and control mice. Student's *t* test, $^{**}P < 0.01$; $n = 14$ to 15 mice per group. (*M*) Representative images of stained arterioles in acute cortical brain slices of $G\alpha_{q/11}^{beKO}$ and control mice before and during stimulation with CO_2. (*N*) Representative traces of diameter measurements in acute cortical brain slices of $G\alpha_{q/11}^{beKO}$ and control mice during stimulation with CO_2. (*O*) Change in arteriolar diameters after stimulation with CO_2 in acute cortical brain slices of $G\alpha_{q/11}^{beKO}$ and control mice (1 arteriole per animal, mean of 3 different sites of each vessel; $n = 5$ to 8 mice per group). Mann–Whitney *U* test, $^*P < 0.05$. (*P*) Baseline diameters of the measured arterioles in acute cortical brain slices of $G\alpha_{q/11}^{beKO}$ and control mice; $n = 5$ to 8 mice per group. Data are means ± SEM.

(Fig. 3 *A*–*C*). However, no changes were seen in the effects of control stimuli (*SI Appendix*, Fig. S6 *A* and *B*) or baseline diameter (Fig. 3*D*). As CO_2-induced blood flow response was impaired in the amygdala, we exposed freely moving mice to 10% CO_2 for 10 min to determine freezing behavior as a measure of the fear response. Confirming its known effect, 10% CO_2 increased freezing in control mice (Fig. 3 *E* and *F*) (16). Even more pronounced was the response of $G\alpha_{q/11}^{beKO}$ mice, which

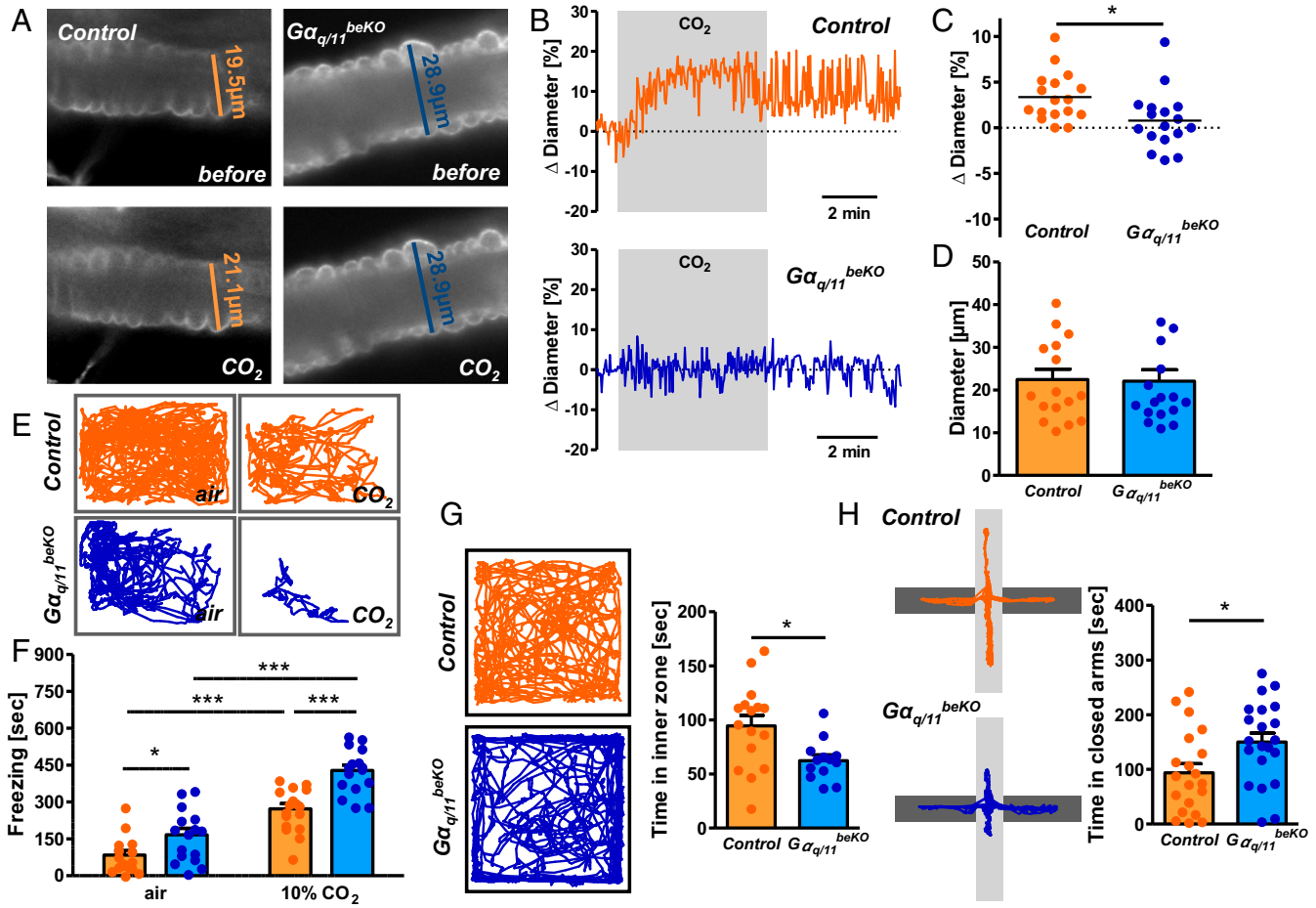

Fig. 3. Impaired vascular reactivity to CO_2 in the amygdala leads to increased fear responses. (*A*) Representative images of stained arterioles in acute amygdala slices of $G\alpha_{q/11}{}^{beKO}$ and control mice before and during stimulation with CO_2. (*B*) Representative traces of diameter measurements in acute amygdala slices of $G\alpha_{q/11}{}^{beKO}$ and control mice during stimulation with CO_2. (*C*) Change in arteriolar diameters after stimulation with CO_2 in acute amygdala slices of $G\alpha_{q/11}{}^{beKO}$ and control mice (1 arteriole per animal, mean of 3 different sites of each vessel, $n = 17$ mice per group). Student's *t* test, $^*P < 0.05$. (*D*) Baseline diameters of the measured arterioles in acute amygdala slices of $G\alpha_{q/11}{}^{beKO}$ and control mice; $n = 17$ mice per group. (*E*) Representative track reports of $G\alpha_{q/11}{}^{beKO}$ and control mice exposed to normal air or CO_2. (*F*) Quantification of freezing behavior during a 10-min normal air or 10% CO_2 exposure in $G\alpha_{q/11}{}^{beKO}$ and control mice. $^*P < 0.05$, $^{***}P < 0.001$ (2-way ANOVA with Bonferroni posttest); $n = 16$ to 17 mice per group. (*G*) Representative track reports of $G\alpha_{q/11}{}^{beKO}$ and control mice during a 10-min open field test and quantification of the time mice spent in the inner zone of the open field arena. Student's *t* test, $^*P < 0.05$; $n = 13$ to 16 mice per group. (*H*) Representative track reports of $G\alpha_{q/11}{}^{beKO}$ and control mice during a 5-min elevated plus maze test and quantification of the time mice spent in the closed arm of the maze. Student's *t* test, $^*P < 0.05$; $n = 13$ to 16 mice per group. Data are means ± SEM.

showed significantly more freezing behavior upon CO_2 exposure than control mice (Fig. 3 *E* and *F*). These findings point to an important influence of vessel reactivity on the chemosensitivity response.

During everyday activities, such as speaking in humans or sniffing in mice, breathing is irregular, resulting in small alterations in blood CO_2/pH and corresponding changes in cerebral perfusion (28). This relationship may explain why freezing behavior was slightly higher in $G\alpha_{q/11}{}^{beKO}$ mice already with normal air (Fig. 3 *E* and *F*). We performed further tests to assess baseline anxiety-like behavior. Open field test and elevated plus maze confirmed a significantly higher anxiety-like behavior in $G\alpha_{q/11}{}^{beKO}$ than in control mice (Fig. 3 *G* and *H*). In contrast, coordination, grip strength, and memory, as well as explorative and hedonic behavior did not differ between genotypes (*SI Appendix*, Fig. S6 *C–G*), indicating that cerebrovascular reactivity is specifically required to regulate the chemosensitive fear and anxiety-like behavior, probably because it compensates for small fluctuations of blood CO_2/pH levels. This mechanism may contribute to the increased anxiety level that is observed in obese humans and animals in which cerebrovascular reactivity is impaired (29, 30).

Impaired Cerebrovascular Reactivity Decreases CO_2-Evoked Respiration and Prolongs Apneic Episodes. Importantly, CO_2 regulates respiration. CO_2 increases breathing frequency and tidal volume by acting on different central areas, most of which are located in the brainstem (31). Direct sensor proteins for increased CO_2/H^+, including GPR4 and TASK2, were identified in neurons of the retrotrapezoid nucleus (RTN) (15). Brainstem neurons that are involved in sensing CO_2 are closely associated with vessels (32, 33), placing them in an ideal position to rapidly sense CO_2 changes. To examine vascular reactivity in the RTN we exposed acute brainstem slices to CO_2, measuring the arteriolar response in the RTN. In contrast to the findings in the cortex and amygdala, RTN arterioles responded to CO_2 with constriction (Fig. 4 *A–C*), revealing opposite vascular reactivity in different brain areas as previously reported in rats (26). Notably, RTN vessels of $G\alpha_{q/11}{}^{beKO}$ mice did not constrict upon CO_2 exposure. As shown already for cortex and amygdala, arterioles of the RTN responded to Ca^{2+} withdrawal and K^+ exposure like control vessels (*SI Appendix*, Fig. S7 *A* and *B*) and had the same baseline diameter (Fig. 4*D*). Thus, CO_2-induced cerebrovascular reactivity depends on endothelial $G\alpha_{q/11}$ signaling in all territories,

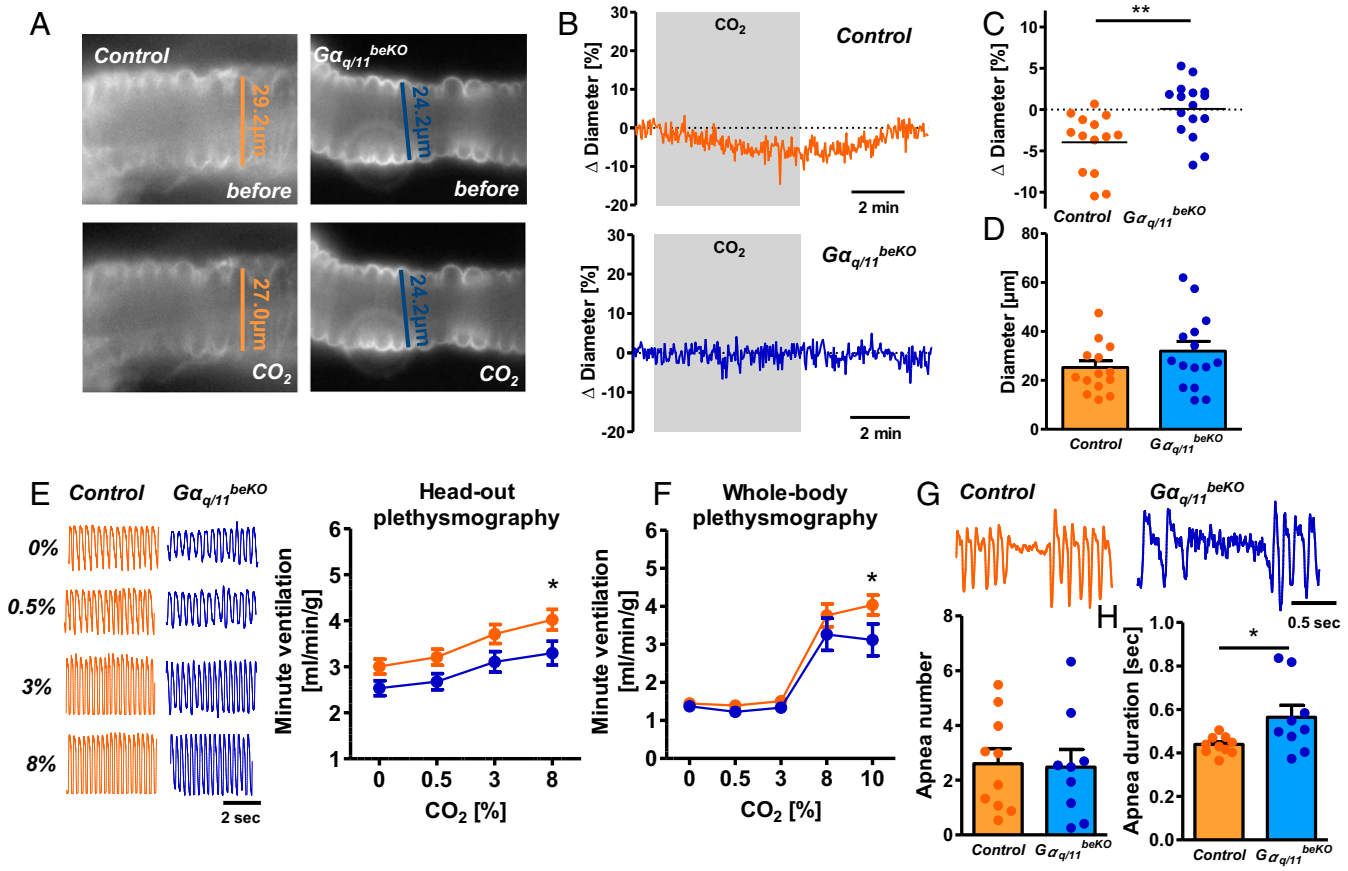

Fig. 4. Impaired vascular reactivity to CO_2 leads to respiratory changes. (*A*) Representative images of stained arterioles in acute RTN slices of $G\alpha_{q/11}{}^{beKO}$ and control mice before and during stimulation with CO_2. (*B*) Representative traces of diameter measurements in acute RTN slices of $G\alpha_{q/11}{}^{beKO}$ and control mice during stimulation with CO_2. (*C*) Change in arteriolar diameters after stimulation with CO_2 in acute RTN slices of $G\alpha_{q/11}{}^{beKO}$ and control mice (1 arteriole per animal, mean of 3 different sites of each vessel). Student's *t* test, $^{**}P < 0.01$; $n = 14$ to 16 mice per group. (*D*) Baseline diameters of the measured arterioles in acute RTN slices of $G\alpha_{q/11}{}^{beKO}$ and control mice; $n = 14$ to 16 mice per group. (*E*) Representative respiratory flow traces of $G\alpha_{q/11}{}^{beKO}$ and control mice exposed to different concentrations of CO_2 and the quantification thereof, recorded by head-out plethysmography. $^{*}P < 0.05$ (RM-ANOVA with Bonferroni posttest). (*F*) Respiratory flow of $G\alpha_{q/11}{}^{beKO}$ and control mice exposed to different CO_2 concentrations, as recorded by whole-body plethysmography. $^{*}P < 0.05$ (RM-ANOVA with Bonferroni posttest); $n = 7$ to 9 mice per group. (*G*) Representative apnea phases of $G\alpha_{q/11}{}^{beKO}$ and control mice recorded by whole-body plethysmography during the inactive period and quantification of the number of apneic phases; $n = 9$ to 10 mice per group. (*H*) Mean duration of all recorded apnea within 1 h during the inactive period of the day for each mouse in $G\alpha_{q/11}{}^{beKO}$ and control mice. Student's *t* test, $^{*}P < 0.05$; $n = 9$ to 10 mice per group. Data are means ± SEM.

although the effects on vessel diameters differ. To evaluate whether the opposing reactivity of RTN and cortical arterioles is specific for CO_2 stimulation, we employed several other vasoactive factors. Sodium nitroprusside, endothelin-1, the thromboxane receptor agonist U46619, and ATP (*SI Appendix*, Fig. S7 *C–F*) had similar effects on the diameter of arterioles in cortex and brainstem slices.

To determine whether the peculiar, CO_2-induced vasoconstriction in the RTN impacts respiration, we measured breathing parameters during CO_2 exposure in awake $G\alpha_{q/11}{}^{beKO}$ and control mice. First, we used a head-out plethysmography setup and exposed control and $G\alpha_{q/11}{}^{beKO}$ mice to different CO_2 concentrations. In contrast to the exaggerated fear response in $G\alpha_{q/11}{}^{beKO}$ mice, changes in ventilation volume per minute upon CO_2 exposure were reduced and not increased in $G\alpha_{q/11}{}^{beKO}$ mice as compared to control mice (Fig. 4*E* and *SI Appendix*, Fig. S8 *A* and *B*). To verify this finding with another method, we assessed respiration by whole-body plethysmography. The respiratory response to CO_2 (10%) was again impaired in $G\alpha_{q/11}{}^{beKO}$ mice (Fig. 4*F* and *SI Appendix*, Fig. S8 *C* and *D*). These differences were also present under normal air conditions (*SI Appendix*, Fig. S8*E*). In summary, the data suggest that the vasoconstrictive effect of CO_2 in the RTN enhances respiratory stimulation while vasodilation in other brain areas counteracts CO_2-induced behavioral responses.

Similar to the fear behavior, we observed a tendency for differing respiration between $G\alpha_{q/11}{}^{beKO}$ and control mice during the plethysmographic recordings already without CO_2 (Fig. 4*E* and *SI Appendix*, Fig. S8 *A–E*). Thus, we examined respiration for a longer period during the inactive phase to detect apneic episodes. We did not find any differences in the incidence of apnea (Fig. 4*G*) but the duration of the apneic periods was longer in $G\alpha_{q/11}{}^{beKO}$ than in control mice (Fig. 4 *G* and *H*), indicating a role of blood flow in reinitiating breathing after a break in respiration. In summary, the data reveal that cerebrovascular reactivity is required to maintain normal respiration and to shorten periods of nonbreathing. Therefore, impaired cerebrovascular reactivity would render patients susceptible to apneic episodes, potentially explaining this complication in diseases like diabetes or obesity (34, 35).

Brain Area-Dependent Vascular Gene Expression Supports Different Regulation of CO_2-Induced Vascular Reactivity. To examine the potential basis for the opposing effects of CO_2 on the vascular reactivity in brainstem compared to other brain areas, we prepared cortical and brainstem vessel fragments of control and

$G\alpha_{q/11}{}^{beKO}$ mice and performed microarrays to determine mRNA expression. The preparations from brainstem and cortex were similar in terms of endothelial marker genes, but we found the mRNA expression of *Nos3* (eNOS) and of genes involved in prostanoid synthesis and sensing to differ significantly between vascular fragments of the cortex and the brainstem (*SI Appendix*, Table S1). None of these genes differed between control and $G\alpha_{q/11}{}^{beKO}$ mice (*SI Appendix*, Table S2).

To characterize the differences between brain areas further, we prepared primary brain endothelial cells from the brainstem and from the subcortical telencephalon (SCT) containing the amygdala (Fig. 5*A*). Cultured cells were almost pure endothelial cells (*SI Appendix*, Fig. S9 *A* and *B*) as described previously for the whole forebrain (14). Interestingly, we found again some changes in the expression of prostanoid-related genes as well as lower expression of the *Nos1* and *Nos3* mRNA in brainstem endothelial cells compared to SCT endothelial cells (*SI Appendix*, Fig. S10*A*). When we stimulated the cells with CO_2, endothelial cells from the brainstem released less NO than the cells from the cortex (Fig. 5*B*), indicating a different reactivity to CO_2. Differences in the release of the prostacyclin derivative $PGF_{1\alpha}$ and PGE_2 were even larger. Brainstem endothelial cells released less of these vasodilative prostanoids in response to CO_2 than SCT endothelial cells (Fig. 5 *C* and *D*). In contrast, the CO_2-induced release of thromboxane A_2, as assessed by TXB_2 concentrations, and the release of $PGF_{2\alpha}$ did not differ between endothelial cells of the SCT and the brainstem (Fig. 5 *E* and *F*). Interestingly, vasodilation of RTN arterioles in response to the prostacyclin analog iloprost was diminished in comparison to arterioles of the cortex (Fig. 5*G*), supporting the role of prostanoids as possibly different between brain areas. All in all, the gene expression data as well as the different release of vasoactive compounds indicate a highly specialized vasculature that supports the functions of the surrounding brain region, such as breathing regulation in the brainstem. In addition, these findings confirm that NO and prostacyclin mediate CO_2-induced vasodilation in the cortex.

Discussion

In this study, we demonstrate a hitherto unknown role of brain endothelial cells in CO_2-induced hyperemia and show that a loss of this cerebrovascular reactivity affects several effects of CO_2 on the central nervous system (CNS). Interestingly, the impaired CO_2 reactivity is associated with dysfunctions in fear and breathing already with atmospheric CO_2 concentrations. The response of the brain vasculature to CO_2 is thought to be mediated by changes in pH rather than in CO_2 or HCO_3^- concentrations (4). In keeping with the role of H^+, GPR4, an endothelial H^+-sensing GPCR, partially mediates the CO_2-induced hyperperfusion in the cortex. GPR4 can activate $G\alpha_{q/11}$ signaling pathways (23) and endothelial $G\alpha_{q/11}$ signaling, as well as GPR4, are instrumental for the CO_2-induced vascular response. These findings also suggest that endothelial cells form the first line of chemosensors, which convert metabolic blood changes rapidly into vascular diameter responses. Endothelial cells in the brain play a crucial role in blood flow reactivity, either by conducted hyperpolarization (36) or the release of vasoactive mediators (37). In line with reports that endothelial-derived vasoactive NO is involved in CO_2-induced CBF increase (38, 39), we found that CO_2 increased NO release in a $G\alpha_{q/11}$-dependent manner. The NO-dependent component of the hypercapnia-induced hyperemia in the brain is strongest at low concentrations of CO_2 (40, 41), which fits our finding that a loss of brain endothelial $G\alpha_{q/11}$ signaling abrogates the CBF response at lower CO_2 concentrations but only partially reduces the response at higher CO_2 concentrations. Whether the released NO is due to eNOS activation is unclear at this stage. Alternatively, the neuronal NO synthase is expressed in endothelial cells and involved in the CO_2-induced perfusion response in the brain (42, 43). In addition to endothelial cells, pericytes, astrocytes, and neurons may contribute to the residual reactivity that still occurred

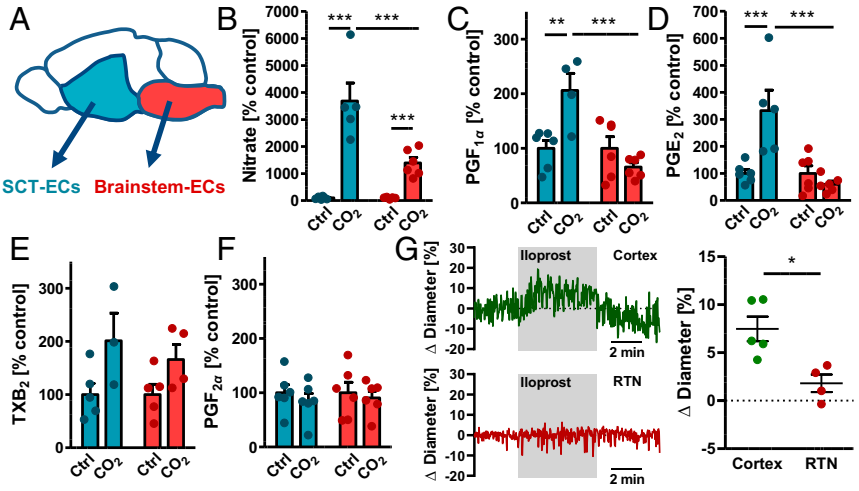

Fig. 5. Release of vasoactive substances differs between subcortical-telencephalic and brainstem endothelial cells. (*A*) Scheme of the brain areas that were used for the preparation of area-specific primary endothelial cells. (*B*) Assessment of NO release by measuring nitrate concentrations in the supernatant of SCT or brainstem endothelial cells after 20-min stimulation with 5% (control) or 15% CO_2. ***$P < 0.001$ (2-way ANOVA with Bonferroni posttest); $n = 4$ to 6 per group, 2 independent experiments. (*C*) $PGF_{1\alpha}$ as a surrogate for prostacyclin release from SCT or brainstem endothelial cells after 20-min stimulation with 5% (control) or 15% CO_2. **$P < 0.01$, ***$P < 0.001$ (2-way ANOVA with Bonferroni posttest); $n = 5$ to 6 per group, 2 independent experiments. (*D*) PGE_2 release from SCT or brainstem endothelial cells after 20-min stimulation with 5% (control) or 15% CO_2. ***$P < 0.001$ (2-way ANOVA with Bonferroni posttest); $n = 5$ to 6 per group, 2 independent experiments. (*E*) TXB_2 as a surrogate for TXA_2 release from SCT or brainstem endothelial cells after 20-min stimulation with 5% (control) or 15% CO_2. $P < 0.05$ for treatment condition in 2-way ANOVA; $n = 3$ to 5 per group, 2 independent experiments. (*F*) $PGF_{2\alpha}$ release from SCT or brainstem endothelial cells after 20-min stimulation with 5% (control) or 15% CO_2; $n = 5$ to 6 per group, 2 independent experiments. Absolute values of prostanoids released by endothelial cells are shown in *SI Appendix*, Fig. S10*B*. (*G*) Representative traces of diameter measurements in acute cortical and RTN brain slices of C57BL/6 mice during stimulation with 1 μM iloprost and quantification thereof (1 arteriole per animal, mean of 3 different sites of each vessel, $n = 3$ mice per group). Student's *t* test, *$P < 0.05$. Data are means ± SEM.

at high CO_2 concentrations in $G\alpha_{q/11}{}^{beKO}$ mice (44–46). Neurons sense pH changes and modulate cerebrovascular reactivity, mediated most likely by the neuronal NO synthase (46). $G\alpha_{q/11}$ signaling in brain endothelial cells not only controls the release of vasoactive molecules, but also the activity of ion channels in capillaries (47, 48) that are involved in the regulation of vascular reactivity (36, 49). The activation of endothelial $G\alpha_{q/11}$ signaling in the brain leads to an arteriolar dilation that depends on NOS activity (50). At the membrane, other, still unidentified endothelial $G\alpha_{q/11}$-coupled receptors might contribute to CO_2-induced cerebrovascular reactivity, but neither GPR68 nor P_2Y_2, both of which are involved in endothelial shear stress responses (13, 20), affected the CO_2-induced perfusion increase.

Currently, the coupling between vessels and neurons is mostly studied in the neuro-to-vascular direction. Conversely, the vascular tone has also a direct impact on neuronal activity in the cortex (51). In support of this idea, our data suggest that impaired CO_2/H^+-induced cerebrovascular reactivity modulates the behavioral and respiratory effects of CO_2. Normal cerebrovascular reactivity apparently attenuates the behavioral effects of CO_2, probably by facilitating its washout from most parts of the brain (*SI Appendix*, Fig. S11). If cerebrovascular reactivity fails to maintain CO_2/H^+ homeostasis in the brain, CO_2-induced fear is unleashed and helps to avoid exogenous CO_2 sources. In contrast, cerebrovascular reactivity seems to retain CO_2 in the RTN, thereby stimulating the CO_2 effect on respiration and enhancing CO_2 elimination from the body. This concept is in line with the recent finding that constriction of local vessels at the ventral medullary surface of the brainstem increases CO_2-induced breathing activity, whereas a decreased respiratory response was observed after local vasodilation (26). The unique features of cerebrovascular reactivity in the RTN could be related to lower production of vasodilatory or an increased release of vasoconstrictive mediators upon CO_2/H^+ stimulation (52). Supporting this idea, we found highly specialized gene expression in vessels of cortex and brainstem. Gene expression favors the synthesis of the vasodilating NO in the cortex or SCT. To assess the endothelial release of vasoactive mediators, we established the primary culture of endothelial cells originating from different brain areas. In these brain area-specific cell populations, CO_2 induced the release of vasodilative factors from endothelial cells of the SCT but not the brainstem. In contrast, CO_2 stimulated the release of thromboxane similarly in both endothelial populations. It was shown before that the synthesis of prostanoids plays a role during hypercapnia-induced perfusion increase (53, 54) and that prostanoids, including the constrictive thromboxane, are released during hypercapnia (54, 55). We conclude that upon CO_2/H^+ stimulation the release of NO and prostanoids differs in the vessels of different parts of the brain but the initial endothelial $G\alpha_{q/11}$-mediated mechanism is the same. It is well described that brain areas respond differently to a hypercapnic stimulus, including negative responses that lead to hypoperfusion (56). In the brainstem, nuclei that are located very close to each other have been described to respond to CO_2 in different ways (26, 56–58). Collectively, all effects seem to serve the goal of removing CO_2 from the brain, with the notable exception of the brainstem (*SI Appendix*, Fig. S11). Importantly, our findings show that specialization of vessels does not only appear along the vascular tree in the brain (10) but also depends on the surrounding brain area.

Impaired cerebrovascular reactivity has an impact on the behavioral and respiratory functions of mice already when breathing normal air, which may be explained by small fluctuations in blood CO_2 concentration during everyday activities, such as sniffing. Similar effects occur during speaking or sighing in humans. These small changes are sufficient to affect both the CBF (28) and the pH in brain extracellular fluids (59), and we have shown that short apneic periods increase cortical perfusion in a $G\alpha_{q/11}$-dependent manner. Thus, short and rapid vascular responses to even small changes in blood CO_2 levels control normal brain function, at least in CO_2-sensitive areas. Impaired cerebrovascular reactivity to CO_2 is a key diagnostic feature of endothelial dysfunction (39) that develops in metabolic syndrome and in several vascular diseases (60). Our data suggest that endothelial dysfunction in the brain contributes to the pathogenesis of sleep apnea and anxiety disorders, and maybe other diseases that are often associated with metabolic syndrome (29, 30, 34). Thus, endothelial dysfunction in the brain and altered cerebrovascular reactivity should be considered as a therapeutic target in several diseases, including metabolic syndrome.

Materials and Methods

Mice. Brain endothelial-specific knockout (beKO) animals were generated by crossing the bacterial artificial chromosome (BAC)-transgenic *Slco1c1-CreER^{T2}* strain (12), which expresses the tamoxifen-inducible CreER^{T2} recombinase under control of the mouse *Slco1c1* regulatory sequences in brain endothelial cells, with mice carrying loxP-flanked alleles. GPR4 and GPR68 whole-genome knockout mice have been described previously (15). All animal experiments were approved by the local animal ethics committee (Regierungspräsidium Karlsruhe; Ministerium für Landwirtschaft, Umwelt und ländliche Räume, Kiel, Germany). For details see *SI Appendix*.

Laser Speckle Imaging. Mice were anesthetized and a small ventilatory tube was inserted into the trachea after tracheotomy and connected to a small animal ventilation device (MiniVent, Harvard Apparatus). Ventilation volume was constant and ventilation frequency was adapted to a physiological expiratory CO_2 concentration of 35 to 45 mmHg that was continuously controlled during the experiments with a capnometer. Laser speckle imaging was performed and regions of interest were set over big cortical vessels. Flux intensities were recorded throughout CO_2 stimulation (10 or 20%, combined with 21% O_2, rest N_2) and normalized to baseline values for each region of interest. For details see *SI Appendix*.

Arteriolar Reactivity in Acute Brain Slices. Vascular reactivity of small arterioles in slices of different brain areas was assessed using a protocol that was described previously (26) with slight changes. For details see *SI Appendix*. Single arterioles were identified in brain slices by typical ring-like labeling (Figs. 2*M*, 3*A*, and 4*A*) and a diameter of >10 μm. RTN slices were taken from the ventral surface below the caudal end of the facial nucleus; amygdala slices were taken 1 to 1.5 mm above the ventral surface of the forebrain and the area between the cortical and thalamic/hypothalamic structures was imaged; cortical vessels were identified in slices taken from the somatosensory cortex.

For further method descriptions see *SI Appendix*.

Data Availability. Microarray data have been deposited in the ArrayExpress database at EMBL-EBI (https://www.ebi.ac.uk/arrayexpress/) under accession number E-MTAB-8521. All other original data files are available from the authors upon request.

ACKNOWLEDGMENTS. We thank W. Häuser (Institute for Experimental and Clinical Pharmacology and Toxicology, University of Lübeck) for help with animal transfer organization, F. Spiecker (Institute for Experimental and Clinical Pharmacology and Toxicology, University of Lübeck) for help with RNAscope experiments, G. Patone and O. Hummel (Max Delbrück Center for Molecular Medicine, Berlin) for help with microarray experiments, and M.-G. Ludwig and K. Seuwen (Novartis) for providing *Gpr4* and *Gpr68* knockout mice. The research leading to these results received funding from the Deutsche Forschungsgemeinschaft (GRK1957 "Adipocyte-Brain Crosstalk"; FOR2372 to E.K.; SCHW 416/5-2 to M.S.), from the European Research Council under the European Union's Horizon 2020 research and innovation programme (grant agreement No. 810331 to M.S.), and the Swiss National Science Foundation (31003A_176125 to C.A.W.).

1. D. Attwell *et al.*, Glial and neuronal control of brain blood flow. *Nature* **468**, 232–243 (2010).
2. K. Kisler, A. R. Nelson, A. Montagne, B. V. Zlokovic, Cerebral blood flow regulation and neurovascular dysfunction in Alzheimer disease. *Nat. Rev. Neurosci.* **18**, 419–434 (2017).
3. G. Burnstock, Purinergic signalling: Therapeutic developments. *Front. Pharmacol.* **8**, 661 (2017).
4. J. E. Brian, Jr, Carbon dioxide and the cerebral circulation. *Anesthesiology* **88**, 1365–1386 (1998).

5. C. S. Roy, C. S. Sherrington, On the regulation of the blood-supply of the brain. *J. Physiol.* **11**, 85–158.17 (1890).
6. M. R. Juttukonda, M. J. Donahue, Neuroimaging of vascular reserve in patients with cerebrovascular diseases. *Neuroimage* **187**, 192–208 (2019).
7. M. L. Ellsworth, T. Forrester, C. G. Ellis, H. H. Dietrich, The erythrocyte as a regulator of vascular tone. *Am. J. Physiol.* **269**, H2155–H2161 (1995).
8. A. V. Gourine, E. Llaudet, N. Dale, K. M. Spyer, ATP is a mediator of chemosensory transduction in the central nervous system. *Nature* **436**, 108–111 (2005).
9. C. Cai *et al*., Stimulation-induced increases in cerebral blood flow and local capillary vasoconstriction depend on conducted vascular responses. *Proc. Natl. Acad. Sci. U.S.A.* **115**, E5796–E5804 (2018).
10. M. Vanlandewijck *et al*., A molecular atlas of cell types and zonation in the brain vasculature. *Nature* **554**, 475–480 (2018).
11. T. Horiuchi, H. H. Dietrich, S. Tsugane, R. G. Dacey, Jr, Analysis of purine- and pyrimidine-induced vascular responses in the isolated rat cerebral arteriole. *Am. J. Physiol. Heart Circ. Physiol.* **280**, H767–H776 (2001).
12. D. A. Ridder *et al*., TAK1 in brain endothelial cells mediates fever and lethargy. *J. Exp. Med.* **208**, 2615–2623 (2011).
13. S. Wang *et al*., $P2Y_2$ and Gq/G_{11} control blood pressure by mediating endothelial mechanotransduction. *J. Clin. Invest.* **125**, 3077–3086 (2015).
14. J. C. Assmann *et al*., Isolation and cultivation of primary brain endothelial cells from adult mice. *Bio Protoc.* **7**, e2294 (2017).
15. N. N. Kumar *et al*., PHYSIOLOGY. Regulation of breathing by CO_2 requires the proton-activated receptor GPR4 in retrotrapezoid nucleus neurons. *Science* **348**, 1255–1260 (2015).
16. A. E. Ziemann *et al*., The amygdala is a chemosensor that detects carbon dioxide and acidosis to elicit fear behavior. *Cell* **139**, 1012–1021 (2009).
17. M. G. Ludwig *et al*., Proton-sensing G-protein-coupled receptors. *Nature* **425**, 93–98 (2003).
18. F. Okajima, Regulation of inflammation by extracellular acidification and proton-sensing GPCRs. *Cell. Signal.* **25**, 2263–2271 (2013).
19. P. S. Hosford *et al*., CNS distribution, signalling properties and central effects of G-protein coupled receptor 4. *Neuropharmacology* **138**, 381–392 (2018).
20. J. Xu *et al*., GPR68 senses flow and is essential for vascular physiology. *Cell* **173**, 762–775.e16 (2018).
21. L. V. Yang *et al*., Vascular abnormalities in mice deficient for the G protein-coupled receptor GPR4 that functions as a pH sensor. *Mol. Cell. Biol.* **27**, 1334–1347 (2007).
22. A. Chen *et al*., Activation of GPR4 by acidosis increases endothelial cell adhesion through the cAMP/Epac pathway. *PLoS One* **6**, e27586 (2011).
23. J. P. Liu *et al*., Each one of certain histidine residues in G-protein-coupled receptor GPR4 is critical for extracellular proton-induced stimulation of multiple G-protein-signaling pathways. *Pharmacol. Res.* **61**, 499–505 (2010).
24. R. Schrage *et al*., The experimental power of FR900359 to study Gq-regulated biological processes. *Nat. Commun.* **6**, 10156 (2015).
25. F. Dabertrand, M. T. Nelson, J. E. Brayden, Acidosis dilates brain parenchymal arterioles by conversion of calcium waves to sparks to activate BK channels. *Circ. Res.* **110**, 285–294 (2012).
26. V. E. Hawkins *et al*., Purinergic regulation of vascular tone in the retrotrapezoid nucleus is specialized to support the drive to breathe. *eLife* **6**, e25232 (2017).
27. D. F. Klein, False suffocation alarms, spontaneous panics, and related conditions. An integrative hypothesis. *Arch. Gen. Psychiatry* **50**, 306–317 (1993).
28. R. G. Wise, K. Ide, M. J. Poulin, I. Tracey, Resting fluctuations in arterial carbon dioxide induce significant low frequency variations in BOLD signal. *Neuroimage* **21**, 1652–1664 (2004).
29. M. Ogrodnik *et al*., Obesity-induced cellular senescence drives anxiety and impairs neurogenesis. *Cell Metab.* **29**, 1061–1077.e8 (2019).
30. A. Shinkov *et al*., Increased prevalence of depression and anxiety among subjects with metabolic syndrome and known type 2 diabetes mellitus - a population-based study. *Postgrad. Med.* **130**, 251–257 (2018).
31. J. You, T. D. Johnson, S. P. Marrelli, R. M. Bryan, Jr, Functional heterogeneity of endothelial P2 purinoceptors in the cerebrovascular tree of the rat. *Am. J. Physiol.* **277**, H893–H900 (1999).
32. S. R. Bradley *et al*., Chemosensitive serotonergic neurons are closely associated with large medullary arteries. *Nat. Neurosci.* **5**, 401–402 (2002).
33. G. Burnstock, Purinergic signaling in the cardiovascular system. *Circ. Res.* **120**, 207–228 (2017).
34. J. A. Chirinos *et al*., CPAP, weight loss, or both for obstructive sleep apnea. *N. Engl. J. Med.* **370**, 2265–2275 (2014).
35. A. A. Tahrani, A. Ali, M. J. Stevens, Obstructive sleep apnoea and diabetes: An update. *Curr. Opin. Pulm. Med.* **19**, 631–638 (2013).
36. T. A. Longden *et al*., Capillary K^+-sensing initiates retrograde hyperpolarization to increase local cerebral blood flow. *Nat. Neurosci.* **20**, 717–726 (2017).
37. G. Guerra *et al*., The role of endothelial Ca^{2+} signaling in neurovascular coupling: A view from the lumen. *Int. J. Mol. Sci.* **19**, E938 (2018).
38. C. Iadecola, Does nitric oxide mediate the increases in cerebral blood flow elicited by hypercapnia? *Proc. Natl. Acad. Sci. U.S.A.* **89**, 3913–3916 (1992).
39. S. Lavi, D. Gaitini, V. Milloul, G. Jacob, Impaired cerebral CO2 vasoreactivity: Association with endothelial dysfunction. *Am. J. Physiol. Heart Circ. Physiol.* **291**, H1856–H1861 (2006).
40. C. Iadecola, F. Zhang, Nitric oxide-dependent and -independent components of cerebrovasodilation elicited by hypercapnia. *Am. J. Physiol.* **266**, R546–R552 (1994).
41. F. M. Faraci, K. R. Breese, D. D. Heistad, Cerebral vasodilation during hypercapnia. Role of glibenclamide-sensitive potassium channels and nitric oxide. *Stroke* **25**, 1679–1683 (1994).
42. Z. Benyó, Z. Lacza, T. Hortobágyi, C. Görlach, M. Wahl, Functional importance of neuronal nitric oxide synthase in the endothelium of rat basilar arteries. *Brain Res.* **877**, 79–84 (2000).
43. Q. Wang, D. A. Pelligrino, V. L. Baughman, H. M. Koenig, R. F. Albrecht, The role of neuronal nitric oxide synthase in regulation of cerebral blood flow in normocapnia and hypercapnia in rats. *J. Cereb. Blood Flow Metab.* **15**, 774–778 (1995).
44. C. N. Hall *et al*., Capillary pericytes regulate cerebral blood flow in health and disease. *Nature* **508**, 55–60 (2014).
45. C. Howarth *et al*., A critical role for astrocytes in hypercapnic vasodilation in brain. *J. Neurosci.* **37**, 2403–2414 (2017).
46. F. M. Faraci *et al*., Acid-sensing ion channels: Novel mediators of cerebral vascular responses. *Circ. Res.* **125**, 907–920 (2019).
47. O. F. Harraz, T. A. Longden, F. Dabertrand, D. Hill-Eubanks, M. T. Nelson, Endothelial GqPCR activity controls capillary electrical signaling and brain blood flow through PIP_2 depletion. *Proc. Natl. Acad. Sci. U.S.A.* **115**, E3569–E3577 (2018).
48. O. F. Harraz, T. A. Longden, D. Hill-Eubanks, M. T. Nelson, PIP_2 depletion promotes TRPV4 channel activity in mouse brain capillary endothelial cells. *eLife* **7**, e38689 (2018).
49. S. K. Sonkusare *et al*., Elementary Ca2+ signals through endothelial TRPV4 channels regulate vascular function. *Science* **336**, 597–601 (2012).
50. C. H. T. Tran, G. Peringod, G. R. Gordon, Astrocytes integrate behavioral state and vascular signals during functional hyperemia. *Neuron* **100**, 1133–1148.e3 (2018).
51. K. J. Kim, J. Ramiro Diaz, J. A. Iddings, J. A. Filosa, Vasculo-neuronal coupling: Retrograde vascular communication to brain neurons. *J. Neurosci.* **36**, 12624–12639 (2016).
52. A. V. Gourine *et al*., Astrocytes control breathing through pH-dependent release of ATP. *Science* **329**, 571–575 (2010).
53. K. Niwa, C. Haensel, M. E. Ross, C. Iadecola, Cyclooxygenase-1 participates in selected vasodilator responses of the cerebral circulation. *Circ. Res.* **88**, 600–608 (2001).
54. L. C. Wagerle, P. A. Degiulio, Indomethacin-sensitive CO2 reactivity of cerebral arterioles is restored by vasodilator prostaglandin. *Am. J. Physiol.* **266**, H1332–H1338 (1994).
55. H. Parfenova, C. W. Leffler, Effects of hypercapnia on prostanoid and cAMP production by cerebral microvascular cell cultures. *Am. J. Physiol.* **270**, C1503–C1510 (1996).
56. P. C. Prokopiou, K. T. S. Pattinson, R. G. Wise, G. D. Mitsis, Modeling of dynamic cerebrovascular reactivity to spontaneous and externally induced CO_2 fluctuations in the human brain using BOLD-fMRI. *Neuroimage* **186**, 533–548 (2019).
57. A. Sato, A. Trzebski, W. Zhou, Local cerebral blood flow responses in rats to hypercapnia and hypoxia in the rostral ventrolateral medulla and in the cortex. *J. Auton. Nerv. Syst.* **41**, 79–86 (1992).
58. R. Wolk, D. Nowicki, J. Sieminska, A. Trzebski, Role of the endogenous nitric oxide in the vasodilatory tone and CO2 responsiveness of the rostral ventrolateral medulla microcirculation in the rat. *J. Physiol. Pharmacol. : Off. J. Pol. Physiol. Soc.* **46**, 127–139 (1995).
59. D. E. Millhorn, F. L. Eldridge, J. P. Kiley, Oscillations of medullary extracellular fluid pH caused by breathing. *Respir. Physiol.* **55**, 193–203 (1984).
60. M. Coucha, M. Abdelsaid, R. Ward, Y. Abdul, A. Ergul, Impact of metabolic diseases on cerebral circulation: Structural and functional consequences. *Compr. Physiol.* **8**, 773–799 (2018).